


Recent developments in the use of geoelectric surveys for investigating causes of road pavement failure: A case study along Darussalam road, Aceh, Indonesia

Muhammad Syukri^{1,2*} , Zul Fadhli², Purwandy Hasibuan³,
Haris Saputra⁴, Rini Safitri¹

¹ Department of Physics, Faculty of Sciences, Universitas Syiah Kuala, Banda Aceh, 23111, Indonesia

² Department of Geophysics Engineering, Faculty of Engineering, Universitas Syiah Kuala, Banda Aceh, 23111, Indonesia

³ Department of Civil Engineering, Faculty of Engineering, Universitas Syiah Kuala, Banda Aceh, 23111, Indonesia

⁴ Department of Civil Engineering, Faculty of Engineering, Universitas Muhammadiyah Aceh, Banda Aceh, 23123, Indonesia

* Corresponding author's e-mail: m.syukri@usk.ac.id

ABSTRACT

This study aims to investigate the lithology of rocks along the Cot Iri Darussalam route to identify the causes of road instability to reduce risks and ensure public safety. The research employed geoelectric resistivity methods, using an ARES resistivity meter for 1D soundings and Geotitis for 2D profiling with a Wenner-Schlumberger configuration. Data were processed with Res2Dinv for 2D inversion and Ipi2win for 1D modeling to derive subsurface resistivity distributions. Results show that Line L1 has resistivity values ranging from 0 to 508.36 Ωm and Line L2 from 0 to 173.56 Ωm , while the 1D soundings (SP1–SP5) range between 1 and 299 Ωm . The lithology consists of wet clay, clay, sandy clay, and sand, with clay-rich layers dominating and interpreted as the main weak zones due to their impermeable and water-saturated nature. These layers, combined with high rainfall, poor drainage, uneven traffic loading, and micro-vibrations from vehicles, are considered the primary causes of road instability in the study area. The study is limited by the number of profiles and the absence of borehole validation, which restricts the precision of lithological correlation, but it highlights the necessity of integrating geophysical and geotechnical approaches for more accurate interpretation. The practical value of this research lies in its contribution to road maintenance and rehabilitation planning in alluvial environments, offering a scientific basis for identifying subsurface weak zones before infrastructure construction. The originality and significance of this work stem from applying resistivity methods to characterize lithological variability and weak layers in an alluvial setting, thereby filling a knowledge gap in understanding road instability mechanisms and providing insights for more resilient transportation infrastructure development in Indonesia.

Keywords: geoelectric, road pavement failure, resistivity, geophysics, environmental.

INTRODUCTION

Road stability is strongly influenced by geological and geotechnical conditions, particularly subsurface lithology. In regions dominated by alluvial deposits and fine-grained sediments, materials tend to weaken when saturated with water, reducing soil strength and accelerating road

degradation. Therefore, investigating subsurface lithology is essential to understand the fundamental causes of road damage and to support sustainable infrastructure planning.

Surface-based assessment methods such as the pavement condition index (PCI) (Nahak et al., 2023; Taufikurrahman et al., 2022) and spatial network analysis including Space Syntax (Van Nes,

2021; Pafka et al., 2020; Zheng et al., 2022) have been widely applied to evaluate road conditions. While effective in documenting surface-level damage, these approaches do not address the geological factors that control road stability. Geophysical techniques, particularly geoelectric resistivity (Syukri et al., 2019) provide insights into lithology and subsurface conditions associated with instability (Fadhli et al., 2025). Previous studies have demonstrated their application for geotechnical problems (Syukri et al., 2022), such as subsurface weakness along Alue Naga Road (Syukri et al., 2020) and landslide-prone zones along the Jantho–Lamno corridor (Saputra et al., 2024). However, the link between resistivity variations, lithological characteristics, and road degradation in alluvial environments remains insufficiently explored.

This urgent research addresses the long-standing road damage along the Cot Iri–Darussalam route. Road instability is a significant geological concern in areas with alluvial deposits, such as Kuta Baro District. Alluvial deposits can lead to weak and unstable subsurface layers due to water. The absorbed water likely comes from roadside drainage channels with poor drainage systems, especially during the rainy season. Fine-grained subsurface layers, such as clay, have a high water absorption capacity, becoming soft, plastic, or liquid (Jahandari et al., 2022; Mahmood et al., 2022). These layers are usually conductive, with low resistivity values, and are considered weak zones on the road (Ademila, 2021; Jekayinfa et al., 2021).

This knowledge gap is highly relevant to the Cot Iri–Darussalam route in Aceh Besar, which is underlain by alluvial deposits and affected by poor drainage conditions. Despite long-standing road problems, no studies have systematically analyzed the role of saturated fine-grained deposits in road instability using resistivity methods. The study is limited by the number of profiles and the absence of borehole validation, which restricts the precision of lithological correlation, but it highlights the necessity of integrating geophysical and geotechnical approaches for more accurate interpretation.

This study aims to investigate the lithology of rocks along the Cot Iri Darussalam route to identify the causes of road instability to reduce risks and ensure public safety. The central hypothesis is that low-resistivity zones correspond to fine-grained, water-saturated materials that significantly weaken the subsurface. This research is significant because it provides a new perspective on the relationship between subsurface lithology and road instability

in alluvial environments. By applying geoelectric resistivity to identify weak, water-saturated layers, the study addresses a gap in understanding that has not been explored in previous road condition assessments. The findings are expected to contribute to the scientific development of geophysical applications in geotechnical studies and offer practical implications for designing more effective and sustainable road infrastructure, particularly in regions with similar geological settings.

GENERAL GEOLOGY OF STUDY AREA

The geology of Aceh Besar is complex and diverse. This region is traversed by the active Semangko Fault, which affects the morphology of Sumatra Island and makes the area prone to earthquakes and landslides (Bennett et al., 1981; Barber et al., 2005). The rocks found in this area include igneous and metamorphic rocks, sedimentary rocks, and ancient volcanic formations. The alluvial deposits in the Krueng Aceh Valley are believed to have been deposited in flood basins, river systems, transitional areas, and linear clastic deposits. Approximately 80% of the rock types in Aceh Besar are alluvial deposits (Qh), while the remainder are Lamteuba volcanic rocks.

Several other formations are present around the study area, including sedimentary and volcanic rocks from the Neogene to Quaternary periods, such as the Lam Teuba Volcanic Formation (QTvt), the Lam Teuba Volcanic Lahar Formation (Qvtl), and the Seulimeum Formation (QTps). The Lam Teuba Volcanic Formation (QTvt) comprises andesite, dacite, pumice breccia, tuff, agglomerate, and volcanic ash and includes lahar rock members (Qvt). The Lahar Member Formation (Qvtl) is a mix of water, volcanic ash, and other materials carried by water flow or rain, characterized by loose and unstable properties. Meanwhile, the Seulimeum Formation (QTps) consists of tuffaceous sandstone, calcareous sandstone, conglomerate, and minor muddy deposits (Bennett et al., 1981; Barber et al., 2005; Muksin et al., 2018; Sieh et al., 2000; McCaffrey et al., 2009).

Based on the geological map (Bennett et al., 1981) shown in Figure 1, the Kuta Baro District in Aceh Besar Regency is predominantly composed of sedimentary rocks with thick alluvial deposits, which are young deposits symbolized by the code Qh. This Qh code indicates the presence of Holocene alluvium deposits

(Simanjuntak et al., 2020). These alluvial deposits contain various materials such as gravel, sand, mud, silty sand, sandy clay, silty clay, and other swamp-derived sediments. The sources of these deposits include volcanic activity from Mount Seulawah Agam and changes in rainfall patterns (Chapkanski et al., 2022).

Alluvial deposits, a significant geological feature in Aceh Besar Regency, especially in Kuta Baro, have characteristics that significantly impact road damage. These deposits are formed from materials transported by river flow or rainfall and consist of various materials, such as gravel, sand, mud, and clay. Alluvial deposits tend to have low consolidation and high water absorption capacity, making them susceptible to erosion and flooding during rainfall. Their strength and stability are also low, making them prone to deformation and soil movement that can lead to road damage (Torres et al., 2021; Choungache et al., 2023; Zhao et al., 2023).

METHODOLOGY

This study consisted of three main stages – data acquisition, data processing, and interpretation.

1. Data acquisition

Field measurements were carried out along the Cot Iri, Darussalam route using two types of equipment: an Automatic Resistivitymeter (ARES) for 1D vertical electrical sounding (VES) and a Geotitis instrument for 2D electrical resistivity tomography (ERT). The Wenner-Schlumberger array was selected because it provides a good balance between vertical and horizontal resolution and is widely applied in engineering geophysics for shallow subsurface investigations (Syukri et al., 2022).

For the 2D geoelectric measurements, line 1 (L1) is 217 meters long with an electrode spacing of 7 meters, while line 2 (L2) is 93 meters long with an electrode spacing of 3 meters. For the 1D geoelectric measurements, Sounding Points 1, 2, 3, 4, and 5 each have a length of 30 meters with an electrode spacing of 0.5 meters. These measurement lines were conducted using the Wenner configuration, aligned with the direction of road instability and located between the road and water channels, as shown in Figure 2. The 2D geoelectric measurement data was processed using Re2dinv and Surfer software to obtain 2D modeling results, which were then interpreted to analyze road instability in the study area. The 1D geoelectric data was processed using Ipi2win

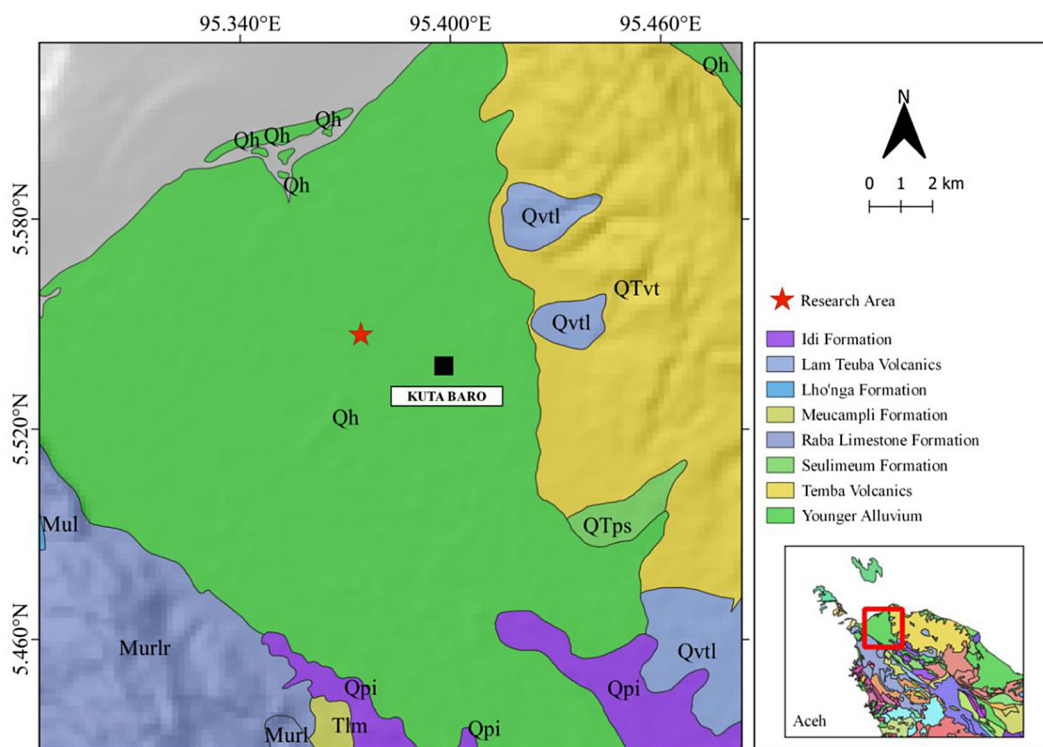


Figure 1. Regional geological map of Aceh Besar (modified from Bennett et al., 1981)

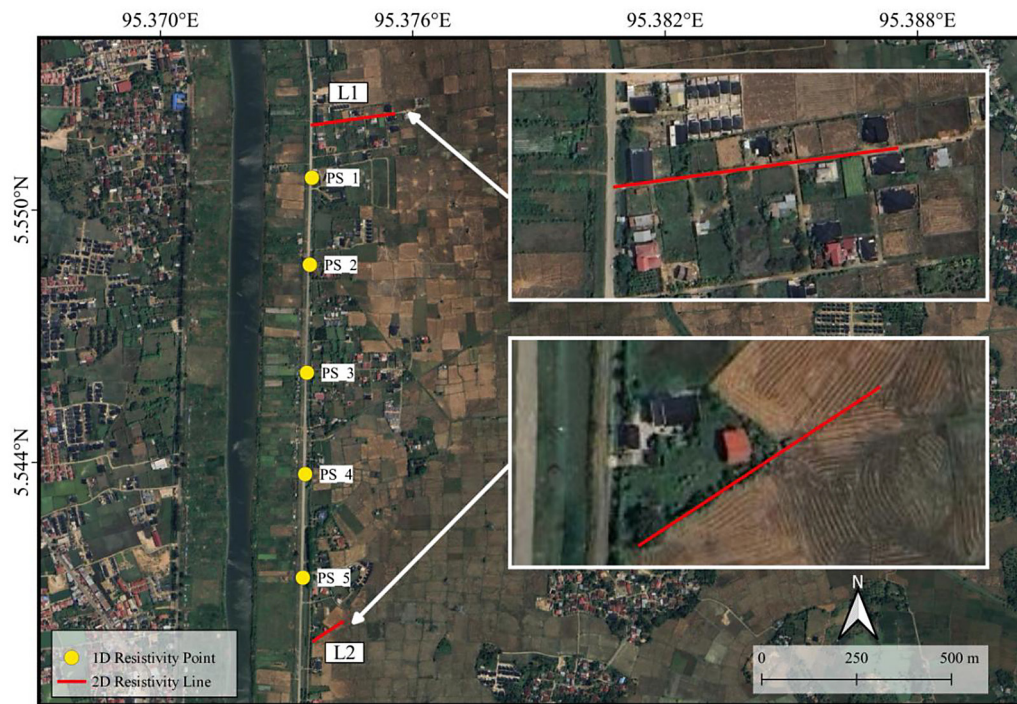


Figure 2. The study area of the geophysical survey

and Surfer software to obtain modeling results as additional data for analyzing road instability in the study area. Layers causing instability can be identified by examining the subsurface resistivity values generated in the cross-sectional modeling, with low resistivity values indicating potential instability.

2. Data processing

The 2D datasets were inverted using Res2D-INV, which applies a least-squares optimization algorithm to convert apparent resistivity measurements into true resistivity cross-sections. The results were visualized and contoured using Surfer to highlight resistivity contrasts. The 1D sounding data were processed with IPI2win, a widely used program for interpreting VES data based on curve matching and inversion routines. The choice of these software packages was motivated by their robustness, wide acceptance in engineering geophysics, and ability to integrate inversion with lithological interpretation.

3. Interpretation

Interpretation was carried out by correlating resistivity values with lithological properties based on published references (Telford et al., 1990; Reynolds, 2011) and local geological information. Low resistivity zones ($< 30 \Omega\text{m}$) were identified as fine-grained, water-saturated

sediments such as clay or silt, which are mechanically weak and prone to instability. Medium resistivity values ($30\text{--}300 \Omega\text{m}$) were attributed to sandy deposits or weathered materials, while high resistivity values ($> 300 \Omega\text{m}$) indicated consolidated rocks or dry coarse sediments. Layers causing road instability were identified specifically as continuous low-resistivity horizons located beneath or adjacent to the roadbed, interpreted as weak water-saturated alluvial deposits.

By integrating 1D and 2D inversion results, the study delineated subsurface zones responsible for instability and provided a reproducible workflow: (i) establish survey geometry, (ii) acquire resistivity data, (iii) invert data using Res2Dinv and IPI2win, (iv) validate resistivity ranges with geological references, and (v) map weak zones related to road deformation.

RESULTS AND DISCUSSION

Resistivity geoelectric measurements were conducted along seven lines, consisting of two 2D lines and five 1D geoelectric points, as shown in Figure 4. The 2D resistivity geoelectric measurements were performed at two locations, namely Lines L1 and L2, using the Wenner-Schlumberger configuration. The measurement data was

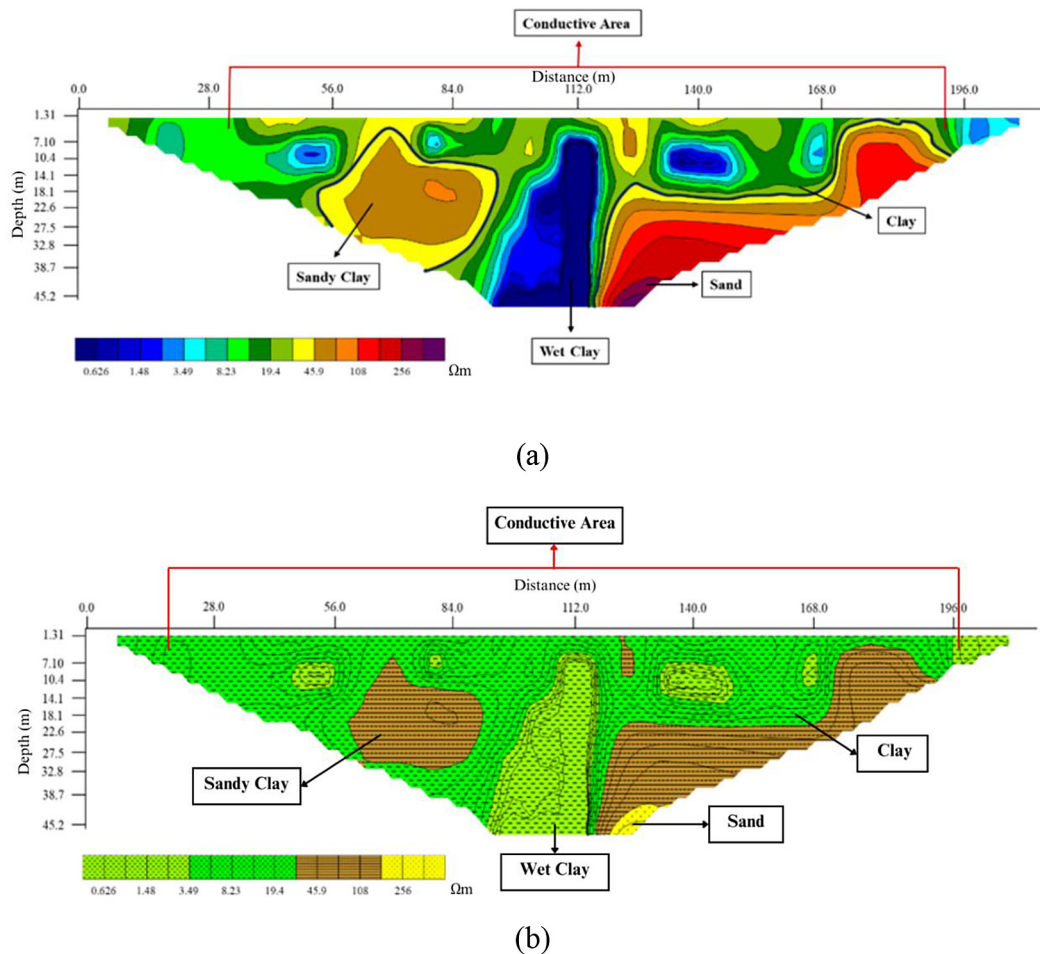


Figure 3. 2D cross-section of survey line L1, (a) Res2Dinv inversion and (b) Surfer visualization, highlighting weak clay zones ($<30 \Omega m$) and stronger sandy clay–sand deposits ($>30 \Omega m$)

processed using Re2dinv software to obtain 2D models, which were then interpreted to analyze road instability in the study area. The 1D geoelectric measurements were conducted using the Wenner configuration in Kuta Baro District, Aceh Besar. The 1D geoelectric data was processed using Ipi2win software to obtain models as supplementary data for analyzing road instability in the study area. The layers causing instability can be identified by examining the subsurface resistivity values in the cross-sectional model, with low resistivity values indicating potential instability.

Line 1 (L1) is located at coordinates $5^{\circ}33'7.72''$ N and $95^{\circ}22'28.64''$ E in Rumpet Village, Kuta Baro District. This line is 217 meters long and situated on a residential road near the unstable road section. The measurement area's elevation at line L1 is 19 meters, with clear weather conditions during data collection. Based on the measurements processed with Res2dinv software, the resistivity model for line L1 is shown in

Figure 3, consisting of resistivity values ranging from 0 to $508.36 \Omega m$ and a penetration depth of 1.31 to 45.2 meters, with four iterations. The resistivity distribution indicates layers of wet clay, clay, sandy clay, and sand, which are part of the alluvial rock formation.

The first deposit has a resistivity value of 3.15 to $24.06 \Omega m$, suspected to be clay deposits, represented by light blue to light green colors. The second deposit has a resistivity range of 0 to $3.14 \Omega m$ and is suspected to be a wet clay deposit, shown in dark blue to blue colors. The third deposit has a resistivity range of 24.07 to $122.43 \Omega m$ and is suspected to be a sandy clay deposit, shown in yellow to red colors. Meanwhile, the fourth deposit has a resistivity range of 183.87 to $508.36 \Omega m$, suspected to be sand deposits, shown in dark red to purple colors.

Based on the resistivity values obtained, Figure 3 also shows the distribution of each type of deposit. First are the clay deposits, which spread

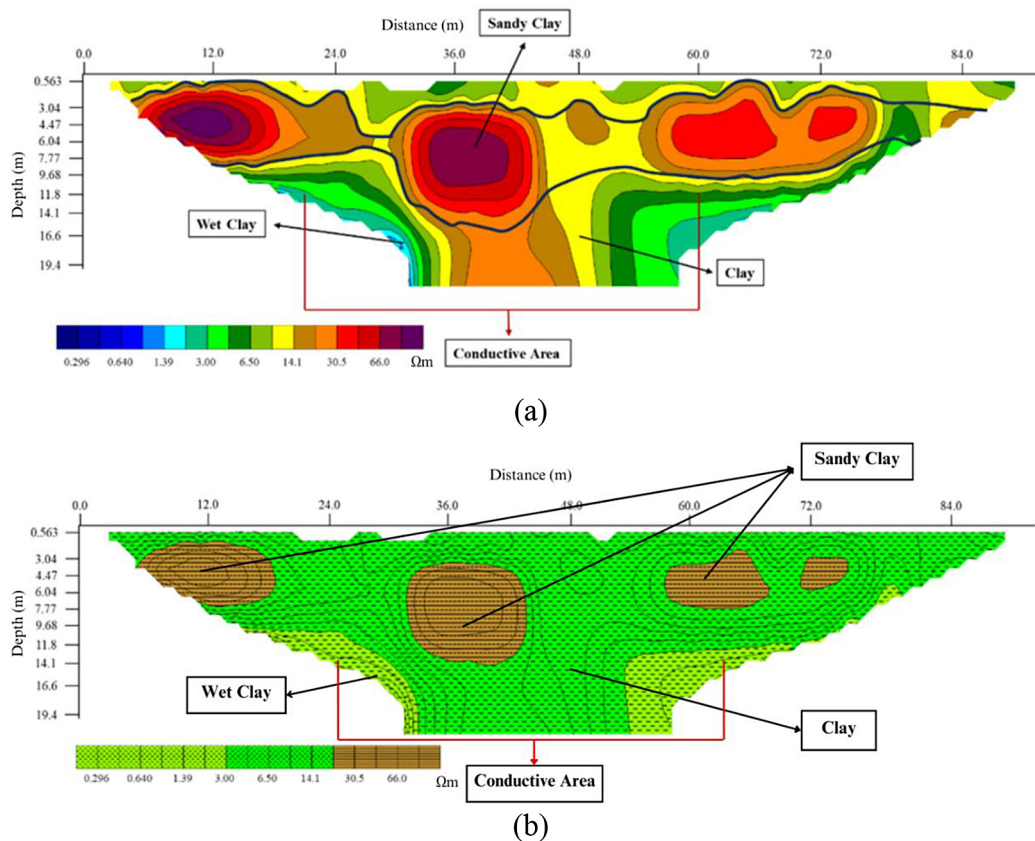


Figure 4. 2D cross-section of survey line L2, (a) Res2Dinv inversion and (b) Surfer visualization, highlighting weak clay zones ($< 30 \Omega m$) and stronger sandy clay–sand deposits ($> 30 \Omega m$)

across the line from 11 to 195 meters, with depths ranging from 1.31 to 45.2 meters. Second, the clay deposits are distributed along the line in intervals of 51 to 57 meters and 79 to 82 meters, with depths of 8.10 to 12.5 meters and 51 to 117 meters. The second clay deposits spread across the line from 131 to 145 meters at depths of 11.4 to 15.5 meters. The last clay deposits are located in intervals of 161 to 166 meters and 196 to 207 meters, at depths of 5.5 to 11.5 meters and 1.31 to 8.5 meters. Third are the sandy clay deposits, distributed along the line from 58 to 89 meters and 120 to 124 meters, at depths of 6.1 to 32.8 meters and 1.31 to 8.5 meters. The second sandy clay deposits are located in intervals of 119 to 178 meters at depths of 3.5 to 45.2 meters. The last deposits, sand, are scattered around the sandy clay and clay deposits, located at intervals of 120 to 126 meters at depths of 37.5 to 45.2 meters.

Line 2 (L2) is located at coordinates $5^{\circ}32'23.85''$ N and $95^{\circ}22'26.21''$ E, in Cot Cut Village, Kuta Baro District, with a measurement area elevation of 18 meters. This line is 96 meters long and situated in a paddy field near the

unstable road. The resistivity model for L2 is shown in Figure 3, consisting of resistivity values ranging from 0.563 to 19.4 meters, with four iterations. The three profiles are depicted based on resistivity values ranging from 0 to $173.56 \Omega m$, with depths from 0.56 to 19.4 meters.

The resistivity distribution for line L2 falls within the range of wet clay, clay, and sandy clay layers, classified as part of the alluvial rock formation. The first deposit has a resistivity value of 4 to $20.72 \Omega m$ and is suspected to be a clay deposit, represented by dark blue to green colors. The second deposit has a resistivity range of 20.73 to $173.56 \Omega m$ and is suspected to be a sandy clay deposit, shown in light green to brown colors. Meanwhile, the third deposit has a resistivity range of 0 to $3 \Omega m$, suspected to be wet clay deposits, indicated by orange to purple colors.

Based on the resistivity values obtained, Figure 4 also shows the distribution of each type of deposit. First are the clay deposits, which spread across the line from 7.5 to 88.5 meters, with depths ranging from 0.56 to 19.4 meters. Second, the sandy clay deposits are located at intervals of

6 to 18 meters, with depths from 2.5 to 7.77 meters. The second sandy clay deposits spread across the line from 32 to 50 meters at depths from 4.9 to 15.4 meters. The third sandy clay deposits are located at intervals of 58 to 68 meters and 70 to 75 meters, with depths from 2.5 to 7.77 meters and 3.9 to 6.6 meters, respectively. The last deposits, wet clay, are located at intervals of 50 to 68 meters and 70 to 77 meters, at depths from 14 to 19.4 meters and 5.5 to 19.4 meters.

The subsurface layers along the two 2D geoelectric lines are dominated by layers with low resistivity values (conductive). The resistivity profile for L1 shows layers with relatively low resistivity ($\rho < 30 \Omega\text{m}$) at depths of 1.31 to 45.2 meters at certain distances. Meanwhile, the resistivity profile for L2 shows low resistivity layers ($\rho < 30 \Omega\text{m}$) at depths of 0.563 to 19.4 meters. Some reasons for the low resistivity values in these locations include water accumulation from rainfall or drainage channels. Field observations indicate that L1 is located in a residential area close to a water channel on the western side and a paddy field on the eastern side, making it likely for water to accumulate in the clay layers in this area. L2 is situated in a paddy field area, which explains the low resistivity values at that location.

Sounding Point 1 is located at coordinates $5^{\circ}33'2.76''$ N and $95^{\circ}22'24.97''$ E, in Cot Cut Village, Kuta Baro District. This line is 30 meters long, perpendicular to the road, and between the unstable road and the water channel. The measurement area's elevation at Sounding Point 1 is 20 meters, with clear weather conditions during data collection. Based on the measurements processed with Ipi2win software, the resistivity model for Sounding Point 1 is shown in Figure 5(a), consisting of three types of curves. The black

curve represents the graph of apparent resistivity values, the red curve represents the synthetic modeling graph, and the blue curve represents the inversion results between field data and the synthetic model regarding actual resistivity values. The resistivity distribution ranges from 2.62 to $138 \Omega\text{m}$, with a penetration depth of 0 to 5.05 meters and an RMS error of 5.79%. The interpretation results shown in Figure 5(b) indicate that the study area's lithology is dominated by two deposits: clay deposits at depths of 0 to 5.05 meters with resistivity values of 2.62 to $26.8 \Omega\text{m}$, and sandy clay deposits at depths greater than 5.06 meters with a resistivity value of $138 \Omega\text{m}$.

Sounding Point 2 is located at coordinates $5^{\circ}32'55.32''$ N, $95^{\circ}22'24.79''$ E. The profile at this location has the same length as that of Sounding Point 1, measuring 30 meters, and runs perpendicular to the road. The distance between Sounding Points 1 and 2 is approximately 230 meters. The elevation at Sounding Point 2 is 21 meters. Data collection was conducted on the same day as at Sounding Point 1, along with Sounding Points 3, 4, and 5. The resistivity model results for Sounding Point 2 are presented in Figure 6(a). This figure consists of three curves: the black curve represents the apparent resistivity values, the red curve indicates the synthetic model, and the blue curve shows the inversion results. The resistivity values range from 1.43 to $135 \Omega\text{m}$, with a penetration depth of 0 to 5.09 meters and an RMS error of 3.12%. The interpretation shown in Figure 6(b) indicates that two types of deposits dominate the lithology of the study area. The first is clay deposits, found at depths of 0 to 2.89 meters and greater than 5.09 meters, with resistivity values between 1.43 and $26.8 \Omega\text{m}$. The second

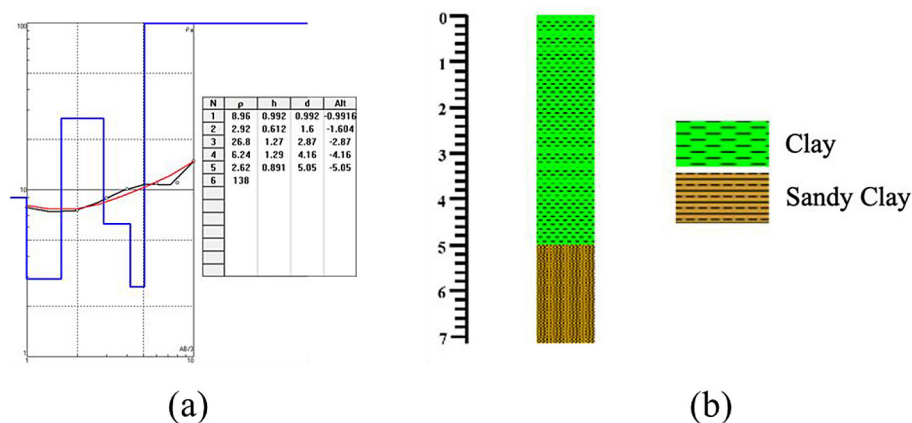


Figure 5. (a) 1D model of Sounding Point 1, (b) interpretation of the 1D section model at sounding point 1

type is sandy clay deposits, located at depths of 2.9 to 5.09 meters, with a resistivity of 135 Ωm .

Sounding Point 3 is located at coordinates 5°32'46.08" N, 95°22'24.54" E. This profile also measures 30 meters long and runs perpendicular to the road. The distance from Sounding Point 2 to Sounding Point 3 is approximately 230 meters. The elevation at Sounding Point 3 is 16 meters. The resistivity model results for Sounding Point 3 are presented in Figure 7(a), which also features three curves: the black curve for apparent resistivity values, the red curve for the synthetic model, and the blue curve for the inversion results. The resistivity values range from 1.47 to 299 Ωm , with a penetration depth of 0 to 5.98 meters and an RMS error of 5.98%. The interpretation presented in Figure 7(b) indicates that two types of deposits dominate the lithology of the study area. The first is clay deposits, found at depths of 0 to 1.96 meters, with resistivity values ranging from 1.47 to 22.5 Ωm . The second type is sandy clay deposits at depths

greater than 1.96 meters, with resistivity values between 40.6 and 299 Ωm .

Sounding Point 4 is located at coordinates 5°32'37.40" N, 95°22'24.39" E. The profile at this point has the same length as the profile at Sounding Point 1 and runs perpendicular to the road. The distance from Sounding Point 3 to Sounding Point 4 is approximately 230 meters, and the elevation of the measurement area at Sounding Point 4 is 18 meters. The resistivity model results for Sounding Point 4 are presented in Figure 8(a), consisting of three curves: the black curve represents the apparent resistivity values, the red curve represents the synthetic model, and the blue curve represents the inversion results. The resistivity values range from 1 to 210 Ωm , with a penetration depth of 0 to 5 meters and an RMS error of 4.01%. The interpretation shown in Figure 8(b) indicates that the lithology of the study area is dominated by two types of deposits: clay deposits, found at depths of 0 to 1.82 meters and greater than 5 meters, with resistivity values between 1 and 10.7 Ωm and sandy

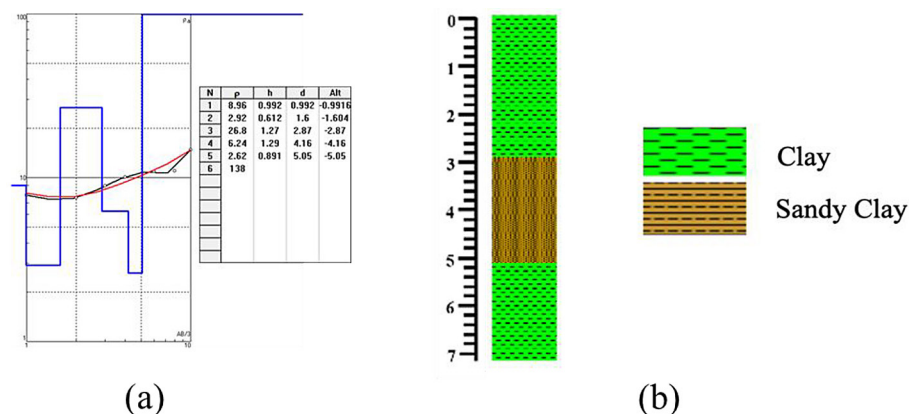


Figure 6. (a) 1D model of Sounding Point 2, (b) interpretation of the 1D section model at sounding point 2

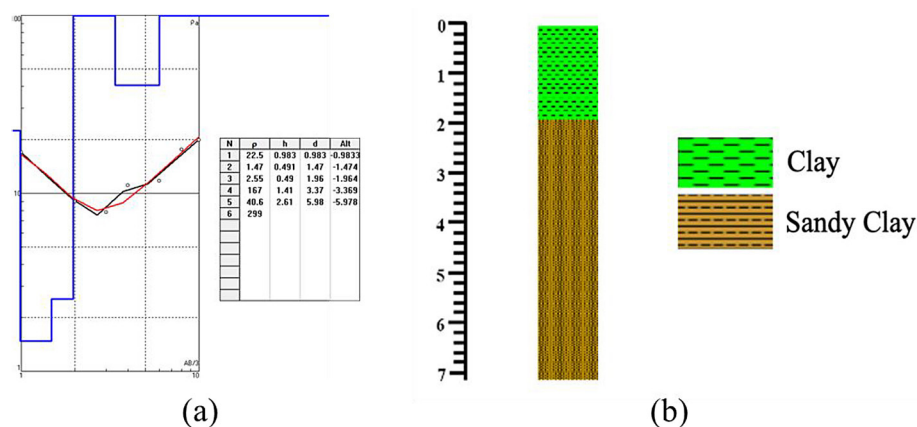


Figure 7. (a) 1D model of Sounding Point 3, (b) interpretation of the 1D section model at sounding point 3

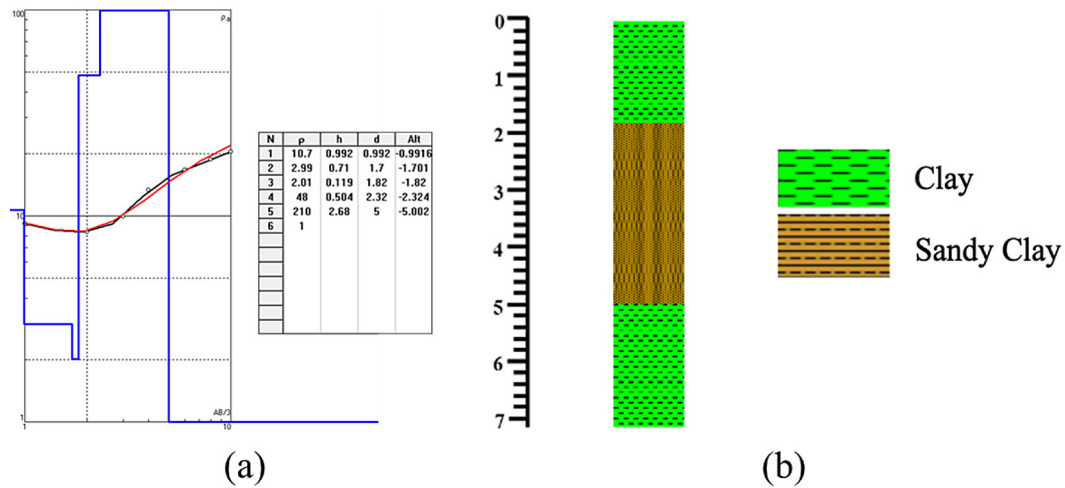


Figure 8. (a) 1D model of Sounding Point 4, (b) interpretation of the 1D section model at sounding point 4

clay deposits, located at depths of 1.83 to 5 meters, with resistivity values ranging from 48 to 210 Ωm .

Sounding Point 5 is located at coordinates 5°32'28.54" N, 95°22'24.19" E. The profile at this point is the same length as that of Sounding Point 1 and runs perpendicular to the road. The distance from Sounding Point 4 to Sounding Point 5 is approximately 230 meters. The elevation of the measurement area at Sounding Point 5 is 18 meters. The resistivity model results for Sounding Point 5 are presented in Figure 9 (a), consisting of three curves: the black curve represents the apparent resistivity values, the red curve represents the synthetic model, and the blue curve represents the inversion results. The resistivity values range from 7.83 to 55.88 Ωm , with a penetration depth of 0 to 5 meters and an RMS error of 1.12%. The interpretation shown

in Figure 9 (b) indicates that the lithology of the study area is dominated by two types of deposits: clay deposits, found at depths of 0 to 3.232 meters with resistivity values between 4.125 and 9.427 Ωm , and sandy clay deposits located at depths greater than 3.232 meters, with resistivity values ranging from 33.13 to 55.88 Ωm .

Figure 10 illustrates the correlation of the 1D section models from the profiles of Sounding Points 1, 2, 3, 4, and 5, which are located between the road and a drainage channel. These five profiles reveal two distinct sedimentary layers: clay and sandy clay. The unstable layer, composed of clay deposits, exhibits low resistivity values ranging from 1 to 26.8 Ωm . Clay is characterized by its impermeable nature, which causes it to absorb water, allowing liquid to penetrate and settle below the surface. Clay becomes elastic and mobile

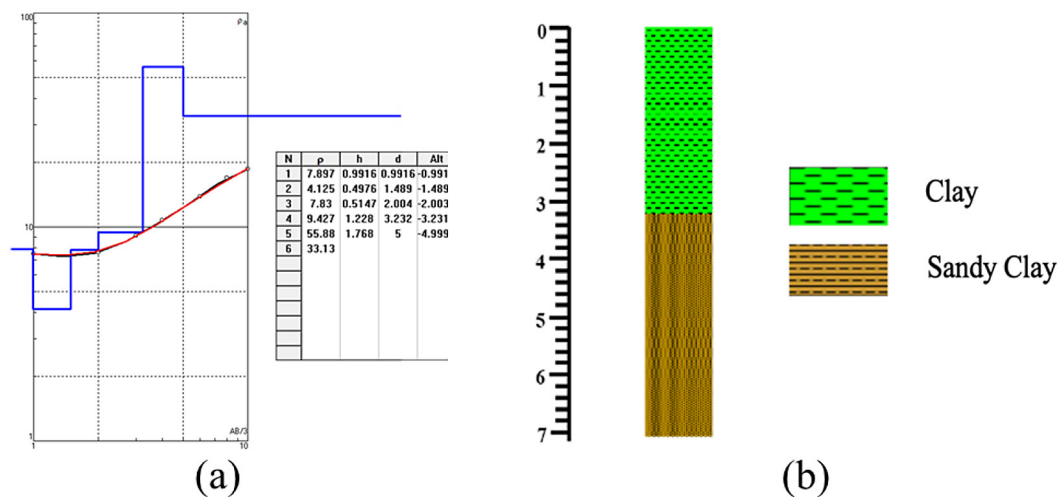


Figure 9. (a) 1D model of Sounding Point 5, (b) interpretation of the 1D section model at Sounding Point 5

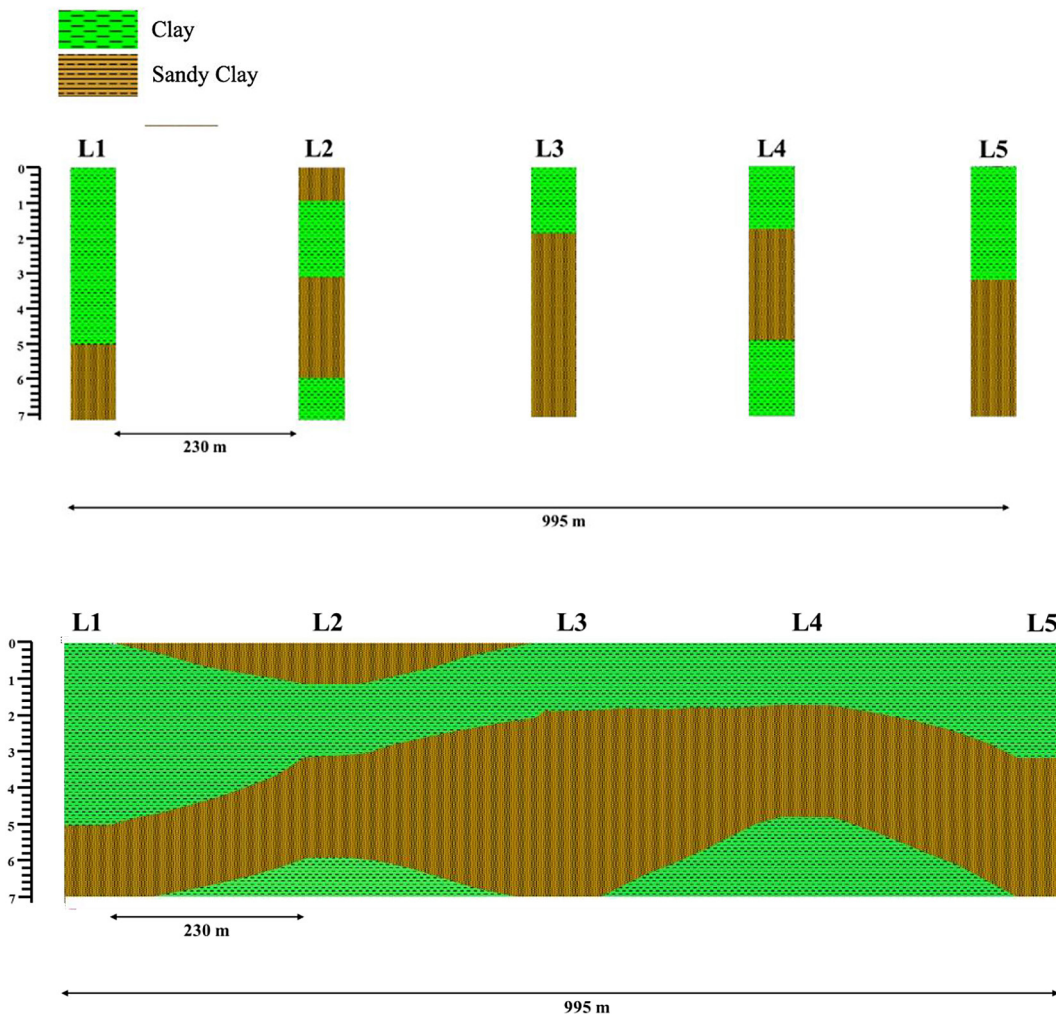


Figure 10. Correlation of 1D sections across profiles L1, L2, L3, L4 & L5

when saturated, leading to surface instability and potential deformation such as cracks, potholes, and undulating roads when subjected to excessive loads (Stempkowska et al., 2022; Lu et al., 2021; Frianeza et al., 2022).

The instability observed in the study area is primarily due to high rainfall and poor drainage systems, which prevent rainwater from effectively channeling away, leading to water accumulation on the road. According to data from the Aceh Provincial Statistics Bureau (2022) (BPS, 2023), there have been several instances of extremely high rainfall over the past few years (data from 2013–2019). High rainfall contributes to water pooling, affecting the roadbed's density. Additionally, inadequate drainage, resulting from improperly constructed water channels, allows the subsurface layers (such as sandy clay) to absorb a portion of the water. In addition to rainfall and drainage issues, excessive loading from

vehicles generates low-magnitude vibrations (microseisms). These microseisms can induce shape changes in wet clay layers due to their softer and less stable nature. Vibrations cause wet clay to experience greater compression or deformation than dry clay. This can lead to subsidence or shifting of the surrounding soil, ultimately causing damage to infrastructure (Smith et al., 2021; Akpila, 2014; Satyanaga et al 2021; Gheshlaghi et al., 2021).

CONCLUSIONS

Research utilizing 1D and 2D resistivity geoelectric methods in the villages of Rumpet and Cot Cut, Kuta Baro District, Aceh Besar Regency, has led to the following conclusions: Line L1 shows a resistivity distribution ranging from 0 to 508.36 Ωm . In comparison, Line L2 ranges from 0 to 173.56 Ωm . In the 1D modeling, Sounding Points

1 through 5 exhibit resistivity values between 1 and 299 Ωm . The lithology of the study area consists of wet clay, clay, sandy clay, and sand, as observed in both the 2D lines and 1D points. The instability of roads in the study area is suspected to be caused by the impermeable nature of clay layers, which become saturated due to high rainfall, water intrusion into drainage channels due to poor drainage systems, excessive loading on one side of the road, and micro-vibrations from vehicles. It is recommended that the number of measurement profiles be increased and the results be correlated with other geophysical methods, such as borehole data, to obtain a more precise and more accurate interpretation.

Acknowledgements

The authors would like to thank the Ministry of Education, Culture, Research and Technology, Indonesia for financial support in the scheme of Penelitian Profesor -PTNBH USK 2022 Grant (Contract no.: 024/UN11.2.1/PT.01.03/PNBP/2022). Special thanks are extended to technical staffs of geophysics laboratory, Geophysics and Physics student, Faculty of Engineering and Faculty of Sciences Universitas Syiah Kuala.

REFERENCES

- Nahak, Y., Pedo, K. S.W. (2023). Identification of road infrastructure damage in East Penfui Village, Kupang Regency. *Timor-Leste Journal of Engineering and Science*, 4, 45–53.
- Taufikurrahman, T., Karyawan, I.D.M.A., Yasa, I.W. (2022). Study of road surface damage due to rainwater puddles using the pavement condition index. *Path of Science*, 8(8), 3010–3018.
- van Nes, A. (2021). The impact of the ring roads on the location pattern of shops in town and city centres. A space syntax approach. *Sustainability*, 13(7), 3927.
- Pafka, E., Dovey, K., Aschwanden, G.D. (2020). Limits of space syntax for urban design: Axiality, scale and sinuosity. *Environment and Planning B: Urban Analytics and City Science*, 47(3), 508–522.
- Zheng, W., Du, N., Wang, X. (2022). Understanding the city-transport system of urban agglomeration through improved space syntax analysis. *International Regional Science Review*, 45(2), 161–187.
- Syukri, M., Saad, R., Anda, S.T., Fadhli, Z. (2019). Resistivity and chargeability signatures of Tsunami Deposits at Aceh Besar and Banda Aceh Coastal Area, Indonesia. *International Journal of Geomate*, 17(59), 133–143.
- Fadhli, Z., Syukri, M., Marvita, Y., Ismail, N, A., Ismail, N, E., Wirsya, E., and Miska, L. (2025). Integration of S-wave value, N-SPT and soil bearing capacity for landslide analysis, *Iraqi Geological Journal*, 58(2B), 36–50.
- Syukri, M., Taib, A. M., Fadhli, Z., Safitri, R. (2020). Geophysical investigation of road failure the case of the main street of Alue Naga, Banda Aceh, Indonesia. In *IOP Conference Series: Materials Science and Engineering* 933(1), 012056. IOP Publishing.
- Saputra, H., Fadhli, Z., Safitri, R., Syukri, M. (2024). Integrated geophysical analysis for landslide risk mitigation: a case study on the weak zone area Of Jantho-Lamno Route, Aceh, Indonesia. *Geomate Journal*, 26(113), 41–49.
- Jahandari, S., Tao, Z., Saberian, M., Shariati, M., Li, J., Abolhasani, M. Rashidi, M. (2022). Geotechnical properties of lime-geogrid improved clayey subgrade under various moisture conditions. *Road Materials and Pavement Design*, 23(9), 2057–2075.
- Mahmood, A., Hassan, R., Fouad, A. (2022). Influence of mellowing periods on short-and long-term performance of lime-treated clay subgrade soils. *International Journal of Pavement Research and Technology*, 15(4), 765–778.
- Ademila, O. (2021). Combined geophysical and geotechnical investigation of pavement failure for sustainable construction of Owo-Ikare highway, Southwestern Nigeria. *NRIAG Journal of Astronomy and Geophysics*, 10(1), 183–201.
- Jekayinfa, S.M., Osinowo, O.O. (2021). Geophysical and geotechnical investigation of road pavement failure in part of Ibadan Metropolis southwestern Nigeria. *Asian Journal of Geological Research*, 4(4), 17–31.
- Bennett, J.D., Bridge, D.McC., Cameron, N.R., Djunuddin, A., Ghazali, S.A., Jeffrey, D.H., Kartawa, W., Keats, W., Rock, N.M.S., Thompson, S.J., and Whandoyo, R. (1981). The Geology of the Banda Aceh Quadrangle, Sumatra (1:250,000), Geological Research and Development Centre, Bandung, 1–2
- Barber, A.J., Crow, M.J., and Milson, J.S. (eds), (2005). *Pre-tertiary stratigraphy, Sumatra: Geology, Resources, and Tectonic Evolution*, Geological Society Memoir: No. 31, London, Geological Society, 41–42.
- Muksin, U., Rusydy, I., Erbas, K., and Ismail, N., (2018). Investigation of Aceh Segment and Seulimeum Fault by using seismological data; a preliminary result, in Proc. *The International Conference on Theoretical and Applied Physics*, 1–5.
- Sieh, K., Natawidjaja, D. (2000). Neotectonics of the Sumatran fault, Indonesia, *Journal of Geophysical Research: Solid Earth*, 105(B12), 28, 295–28, 326.
- McCaffrey, R. (2009). The tectonic framework of

- the Sumatran subduction zone, *Annual Review of Earth and Planetary Sciences*, 37(1), 3.1–3.22.
19. Simanjuntak, A. V. H., Asnawi, Y., Umar, M., Rizal, S., dan Syukri, M. (2020). A microtremor survey to identify seismic vulnerability around Banda Aceh using HVSR analysis. *Elkawanie*, 6(2), 342–358.
 20. Chapkanski, S., Brocard, G., Lavigne, F., Tricot, C., Meilianda, E., Ismail, N., Majewski, J., Goiran, J. P., Alfian, D., Daly, P., Horton, B., Switzer, A., Degroot, V., Steuer, A., Siemon, B., Caverro, J., Vermoux, C., dan Darusman, D. (2022). Fluvial and coastal landform changes in the Aceh River delta (northern Sumatra) during the century leading to the 2004 Indian Ocean tsunami. *Earth Surface Processes and Landforms*, 47(5), 1127–1146. <https://doi.org/10.1002/esp.5292>
 21. Torres, E.S., Adajar, M.A.Q. (2021). Geotechnical characterization of alluvial soil as an alternative roadway construction material. *GEOMATE Journal*, 20(81), 125–131.
 22. Choungache, B., Zaitri, R. (2023). Influence of the incorporation of alluvial sand on the mechanical behavior of marl soil. *Engineering, Technology & Applied Science Research*, 13(2), 10363–10366.
 23. Zhao, G., Guo, W., Li, X. (2020). Mechanical properties of mega-thick alluvium and their influence on the surface subsidence. *Geotechnical and Geological Engineering*, 38, 137–149.
 24. Syukri, M., Anda, S.T., Umar, M.,... Fadhli, Z., Safitri, R. (2022). Identification of Tsunami Deposit at Meulaboh, Aceh (Indonesia) Using Ground Penetrating Radar (GPR) *International Journal of Geomate* Open source preview, 23(96), 171–178.
 25. Telford, W.M., Geldart L.P. (1990). *Applied Geophysics Second Edition*. Cambridge University Press: United Kingdom
 26. Reynolds, J. M. (2011). *An introduction to applied and environmental geophysics*. John Wiley & Sons.
 27. Stempkowska, A., Wójcik, Ł., Ostrowski, K. A., Gawenda, T. (2022). Low-energy clay–cement slurries find application as waterproofing membranes for limiting the migration of contaminants—case studies in Poland. *Energies*, 16(1), 230.
 28. Lu, Y., Liu, S., Zhang, Y., Yang, M., Fu, Z., Wang, L. (2021). Sustainable reuse of coarse aggregates in clay-based impervious core: compactability and permeability. *Journal of Cleaner Production*, 308, 127011.
 29. Frianeza, C., and Adajar M. A. (2022). Effectiveness of compacted polyurethane-clay as a sanitary landfill liner. *Geomate Journal* 23(100), 142–148.
 30. Badan Pusat Statistik (2023). *Population of Indonesia by Province 2017, 2018, 2019, 2020, and 2021*. Retrieved from <https://www.bps.go.id/linkTabelStatis/view/id/1267> on October 26, 2024
 31. Smith, I. (2021). *Smith's elements of soil mechanics*. John Wiley & Sons.
 32. Akpila, S. B. (2014). Bearing capacity and settlement response of raft foundation on sand using standard penetration test method. *SENRA Academic Publishers, British Columbia. Canadian Journal of Pure & Applied Sciences*, 8, 2769–2774.
 33. Satyanaga, A., Wijaya, M., Zhai, Q., Moon, S. W., Pu, J., Kim, J. R. (2021). Stability and consolidation of sediment tailings incorporating unsaturated soil mechanics. *Fluids*, 6(12), 423.
 34. Gheshlaghi, F., Mardani, A. (2021). Prediction of soil vertical stress under off-road tire using smoothed-particle hydrodynamics. *Journal of Terramechanics*, 95, 7–14.